J Solid State Electrochem (2002) 6: 522–527
DOI 10.1007/s10008-002-0267-6

ORIGINAL PAPER

V. Vivier · C. Cachet-Vivier · A. Regis · G. Sagon
J.-Y. Nedelec · L.T. Yu

Electrochemical study of the degradation kinetics of polyaniline powder in sulfuric and hydrochloric acid media

Received: 17 September 2001 / Accepted: 18 January 2002 / Published online: 27 April 2002

Abstract Investigation of the degradation kinetics of polyaniline (PANi) powder has been performed with a cavity microelectrode in sulfuric and hydrochloric acid electrolytes using cyclic voltammetry. It was shown that the overall degradation mechanism is limited by first-order reaction kinetics. The rate constant of the polymer hydrolysis was found to be lower than the one determined for thin films. The influence of the electrolyte concentration was also investigated and compared with our previous work on the use of PANi as a battery material.

Keywords Cavity microelectrode · Polyaniline · Polymer degradation · Cyclic voltammetry

Introduction

Conducting organic polymers exhibit noteworthy reversible electrochemical behavior. Among them, polyaniline (PANi) has been intensively investigated during these last decades [1] because of the wide variety of possible applications, such as solid state transistors [2], biological microsensors [3] or battery electrode materials [4, 5, 6]. The electrochemical behavior of PANi is based on three oxidation states, the so-called leucoemeraldine (reduced form), emeraldine (neutral form), and pernigraniline (fully oxidized form), which can be independently synthesized via chemical methods as already described many decades ago [7].

Numerous studies have been done to elucidate the mechanism that occurs for each electrochemical step [8, 9, 10, 11, 12, 13]. Considering the couple leucoemeraldine/emeraldine, it is now generally agreed that this mechanism is coupled with proton expulsion at low pH values, whereas anion incorporation is involved at higher pH values. However, Barbero et al. [14] have shown that non-negligible anion exchange also occurs at low pH values ($\mathrm{pH} < -1$).

PANi is easily electropolymerized as a thin film on a metallic electrode, and many electrochemical investigations are related to such films [1, 15, 16, 17]. Conversely, little attention has been paid to the electrochemical performance of powder material, and only a few studies have been performed on PANi powder with the use of a graphite paste electrode [18, 19, 20, 21]. Moreover, the scan rates that can be used in cyclic voltammetry with such a composite electrode must be very slow and cannot exceed a few millivolts per second. The recent development of techniques allowing work with microquantities of powder materials offers new possibilities to study solid state reactions [22, 23, 24, 25, 26, 27, 28]. Among them, we developed the cavity microelectrode (CME), which needs only few nanograms of material [26, 27, 28]. Similarly with an usual microelectrode used for studying soluble compounds [29, 30], the ohmic drop Ri and the time constant RC_d (ascribable to capacitive currents) are considerably reduced because of the small dimensions of the cavity volume of the CME. Thus, high scan rates (over 100 V s^{-1} [26]) can be easily reached. In addition, it is possible to study the kinetics of solid state reactions of powder materials. In this paper, we report the kinetic study of the degradation of PANi powder when an oxidative potential is applied.

Experimental

Synthesis

Polyaniline was chemically synthesized according to the protocol previously described [18, 19]. An aniline solution (0.5 mol L^{-1}) was

V. Vivier (✉) · C. Cachet-Vivier · J.-Y. Nedelec · L.T. Yu
Laboratoire d'Electrochimie,
Catalyse et Synthèse Organique,
UMR 7582 CNRS,
Université Paris Val de Marne,
2 Rue H. Dunand, 94320 Thiais, France
E-mail: vivivier@ccr.jussieu.fr

A. Regis · G. Sagon
Laboratoire de Dynamique,
Interactions et Réactivité,
UMR 7075 CNRS, Université Paris 6,
2 Rue H. Dunant, 94320 Thiais, France

oxidized with ammonium persulfate (0.5 mol L^{-1}) in a sulfuric acid medium. During the reaction the temperature was kept at 278 K. A dark-blue precipitate was isolated, washed with a 1 mol L^{-1} H_2SO_4 solution and finally dried under dynamic vacuum for ca. 48 h. PANi powder was stored in a closed bottle in an air atmosphere. The overall formula, $C_{24}H_{20}N_4O_4S$, was identified from elemental analysis, which corresponds to the sulfate emeraldine salt:

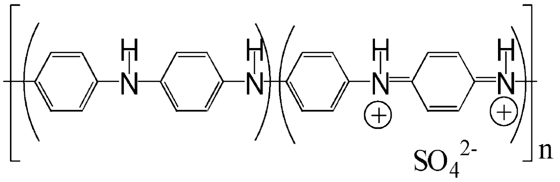

For the studies in hydrochloric acid, the sulfate ions were removed by passing a large amount of 1 mol L^{-1} HCl solution over the emeraldine powder. The resulting product was identified as $C_{24}H_{20}Cl_2N_4$.

Electrochemical measurements

Electrochemical measurements were carried out within a classical three-electrode cell. The working electrode was a CME schematized in Fig. 1. The diameters of the cavity of the electrodes used were 25 and 50 μm, the depth of which were 12 and 20 μm, respectively (for a detailed description of this electrode, see [26, 27, 28]). The cavity was filled with pure material grains (i.e. without any adjunction of additives such as graphite or carbon black) using the electrode as a pestle.

As one of the redox states of PANi is a good electronic conductor [18, 19], no graphite or carbon has to be added to perform the electrochemical measurements. After electrochemical studies, the microcavity is emptied by washing it with an ultrasonic cleaner at 50 °C in hydrogen peroxide (30%) for 5 min. Background scans of the Pt wire were recorded in 0.5 mol L^{-1} H_2SO_4 before each experiment to verify the cleanness of the cavity. An optical microscope (Olympus BX30) coupled to a numerical camera unit (DP10) was used to control the included material before and after the electrochemical experiments.

The reference and the counter electrodes were a saturated calomel electrode (SCE) and a 1 cm^2 area Pt plate, respectively. Electrochemical measurements were performed using an Autolab PGSTAT 30 potentiostat.

Raman device

The Raman spectrometer was a Dilor XY device equipped with a liquid nitrogen cooled CCD detector with black illumination and an optical microscope, which allowed the laser to be focused on a 1 μm^2 surface area.

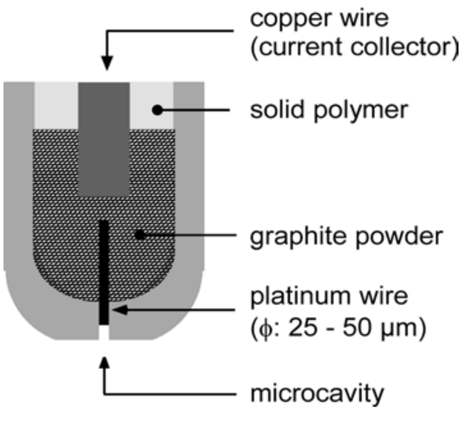

Fig. 1. Schematic representation of the apex of a cavity microelectrode

Results and discussion

Cyclic voltammetry

In Fig. 2, cyclic voltammograms at 20 and 200 mV s^{-1} recorded with PANi powder included in a 25 μm diameter CME are shown. The shape of these curves are very similar to these obtained on PANi thin films or with a PANi carbon paste composite electrode in acidic media. Peaks labeled A1 and C1 correspond to the emeraldine/leucoemeraldine couple, for which the global mechanism involves one proton per electron exchanged [1] with a total exchange of two electrons per PANi unit. The capacitive current observed is consistent with the transition from a conducting form (emeraldine) to an insulating form (leucoemeraldine) [1, 18]. From the value of the exchanged charge and the cavity dimensions, and taking into account that the charge does not vary with respect to the scan rate, one can assume that all the PANi included in the cavity participates in the electrochemical reaction. The total capacitive charge evaluated from these curves is quite similar to the Faradic charge.

By extending the scan range toward more positive potentials (Fig. 3), two new peaks (A2 and C2) corresponding to the emeraldine/pernigraniline couple at about 0.6 V/SCE appear. During subsequent cycles, both electrochemical responses progressively disappear. This behavior corresponds to polymer degradation, as already mentioned for thin films [31, 32, 33].

In situ Raman spectroscopy characterization

The formation of each oxidation state of PANi was characterized in situ by Raman microspectrometry, as presented in Fig. 4. No significant modification of the

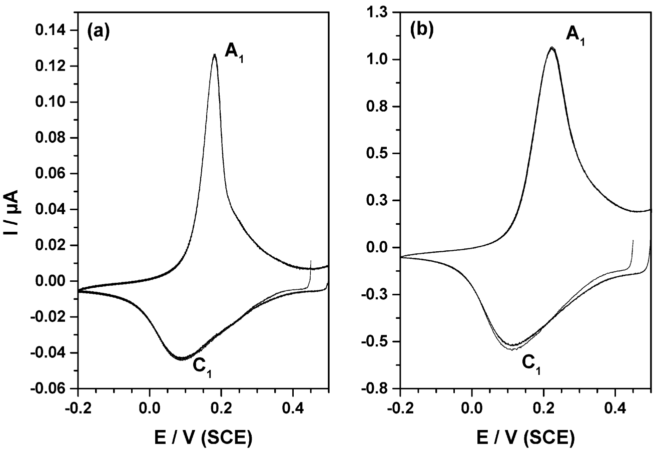

Fig. 2. Cyclic voltammograms recorded with a CME (25 μm diameter) in a 0.5 mol L^{-1} H_2SO_4 solution at 20 mV s^{-1} (**a**) and 200 mV s^{-1} (**b**). Peaks A_1/C_1 correspond to the system leucoemeraldine/emeraldine

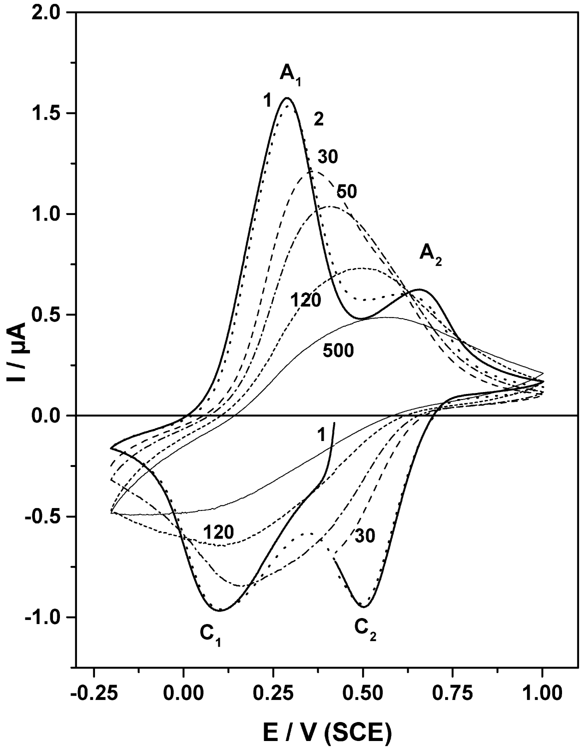

Fig. 3. Evolution of cyclic voltammograms versus the number of cycles recorded with a CME (50 µm diameter) in a 0.5 mol L^{-1} H_2SO_4 solution at 50 mV s^{-1}. Peaks A_1/C_1 and A_2/C_2 correspond to the system leucoemeraldine/emeraldine and emeraldine/pernigraniline, respectively

Raman spectra was noticed between the dried powder included in the cavity of the microelectrode (Fig. 4a) by comparison with the same electrode immersed in a 0.5 mol L^{-1} sulfuric acid solution at rest potential (Fig. 4b). All the observed vibration modes can be attributed to PANi [34, 35, 36, 37]. The two most intense vibration bands located at 1624 and 1196 cm^{-1} correspond to the vibration of C-C and C-H bonds of the aromatic groups. In both cases, a broad band is observed at 1340 cm^{-1}, indicating that the structure is protonated, which is in good accordance with the synthesis protocol and the solution pH for the in situ experiment. Moreover, the 1055 cm^{-1} band observed for both spectra corresponds to SO_4^{2-} counter ions that derive from the synthesis of PANi and from the electrolytic solution used for the electrochemical study. After applying a –0.2 V/SCE potential for 1 min, the Raman spectrum becomes characteristic of leucoemeraldine (Fig. 4c), and is very similar to that of emeraldine. After 1 min polarization at –1 V/SCE, the formed product is pernigraniline (Fig. 4d). Furthermore, in the 1200–1600 cm^{-1} range the strong parasitic background can be attributed to polymer degradation.

Kinetics of degradation of PANi

From the cyclic voltammograms presented in Fig. 3 and the Raman spectrum in Fig. 4d, we deduce that PANi degradation occurs at potentials higher than 0.5 V/SCE, as mentioned for thin films [31, 32]. This reaction can be considered as hydrolysis of a Schiff base [31, 32, 38], leading to the formation of *p*-benzoquinone (BQ) [32]. The overall hydrolysis mechanism should involve several successive elementary steps, which can be decomposed as follows:

$$(\mathrm{PANi})_n^{\mathrm{red}} \underset{-4e-4H^+}{\overset{+4e+4H^+}{\rightleftharpoons}} (\mathrm{PANi})_n^{\mathrm{ox}} \tag{1}$$

$$(\mathrm{PANi})_n^{\mathrm{ox}} \xrightarrow[k_{\mathrm{obs}}]{+2H_2O,\ -\ NH_3} (\mathrm{PANi})_{n-1}^{\mathrm{ox}} + \mathrm{BQ} \tag{2}$$

where $(\mathrm{PANi})_n^{\mathrm{red}}$ and $(\mathrm{PANi})_n^{\mathrm{ox}}$ are the reduced and the oxidized forms, respectively. The subscript n is related to the polymer length and k_{obs} is the measurable degradation kinetic constant that we intend to determine. Assuming that the reaction kinetics is a first-order reaction with respect to the BQ concentration, variations of the concentration are given by:

$$\frac{\mathrm{d(BQ)}}{\mathrm{d}t} = k_{\mathrm{obs}}(\mathrm{PANi})_n^{\mathrm{ox}} \tag{3}$$

Measurement of the total charge exchanged at the end of each oxidation sweep allows evaluation the amount of PANi that was not degraded and thus to evaluate the amount of BQ formed. The duration of the hydrolysis was evaluated from both the scan rate applied and the potential range in which the hydrolysis can occur. For the latter, we assumed that the hydrolysis can take place as soon as the first amount of pernigraniline is electrogenerated, i.e. for potentials higher than 0.5 V/SCE.

Variation of the number of moles of non-degraded PANi versus time is shown in Fig. 5, when performing cycles in 0.5 mol L^{-1} H_2SO_4 at 50 and 100 mV s^{-1} in the –0.2 to 1 V/SCE potential range. In both cases, we observe a linear decrease of the PANi amount (in a semi-log scale), corroborating the assumption of a first-order kinetics mechanism involved in the limiting step of the degradation reaction. From the slopes of each curve, the kinetic constants are evaluated and are found to be 0.9×10^{-3} and 10^{-3} s^{-1} for $v = 50$ and 100 mV s^{-1}, respectively. These values can be considered as independent of the scan rate, and are about 10 times lower than those obtained by Stilwell and Park [32] on thin films. Such a difference can be explained by the difference in the texture microstructure between powder and film materials. These authors [32, 39] observed a hydrolysis rate decrease when the thickness increased; this can be explained by the transition of a dense polymeric structure to a fiber-like structure with film thickness. As a result, our numerical values cannot be directly compared with the literature one obtained on thin polymerized films.

In more concentrated sulfuric acid solution (Fig. 6), the rate constant of PANi degradation is increased. For a 1 mol L^{-1} H_2SO_4 solution, k_{obs} is ca. 1.6×10^{-3} s^{-1} (instead of 0.9×10^{-3} s^{-1} for 0.5 mol L^{-1} H_2SO_4). It

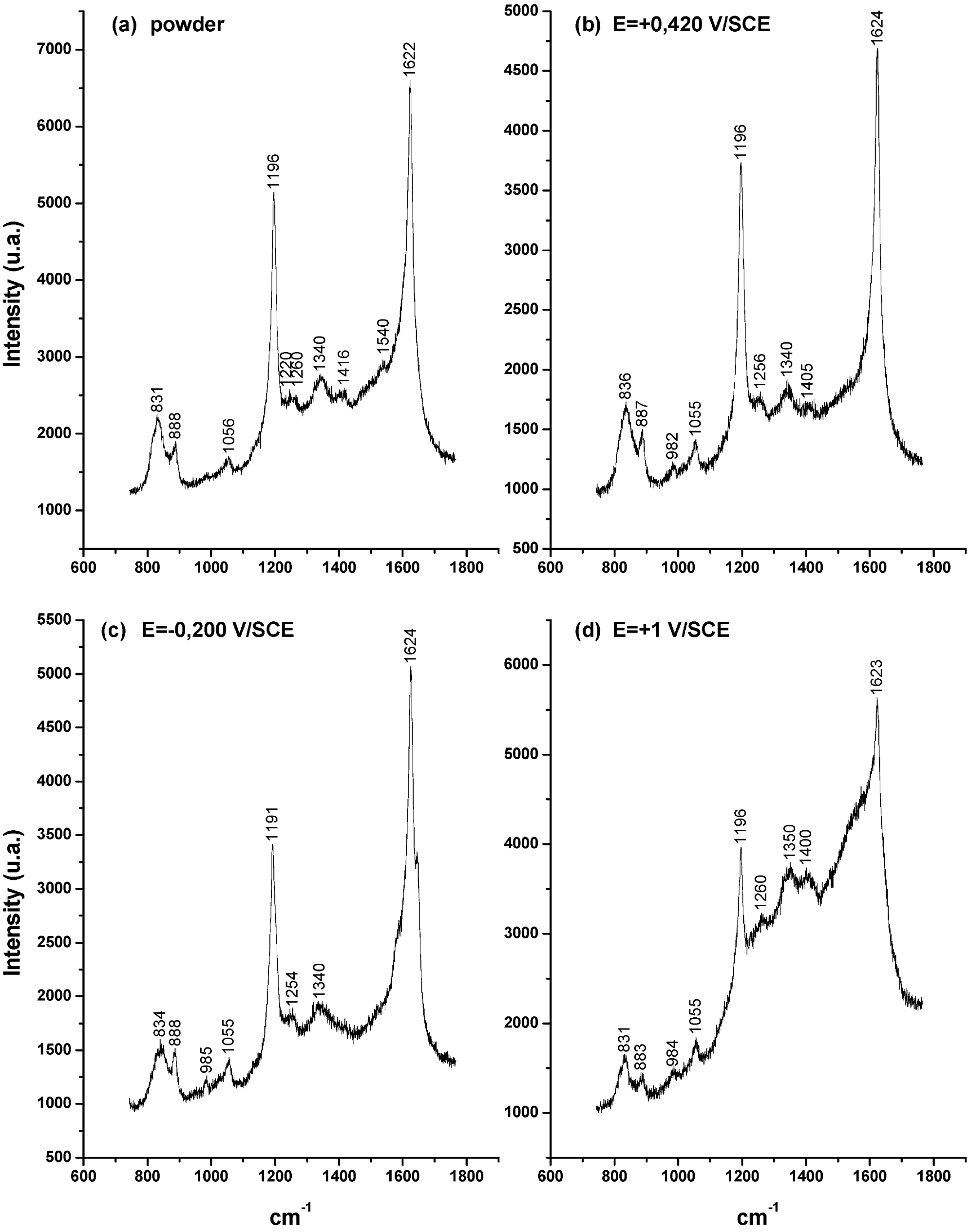

Fig. 4. Raman spectra recorded on PANi powder (**a**), at rest potential (0.42 V/SCE) (**b**), after 1 min polarization at –0.2 V/SCE (**c**), and after 1 min polarization at +1 V/SCE (**d**). Experiments (**b**)–(**d**) were performed in situ in a 0.5 mol L^{-1} H_2SO_4 solution

reaches 2.5×10^{-3} s^{-1} for a 2 mol L^{-1} H_2SO_4 solution. The evolution of the rate constant is consistent with the literature data [32, 40]. It can explain the capacity loss observed when cycling the leucoemeraldine/emeraldine system in different H_2SO_4 solutions [41], for which the capacity loss is higher in more concentrated acids than for more diluted solutions. Indeed, it was shown that even if limiting the potential range below 0.5 V/SCE, a very small amount of PANi was nevertheless transformed into pernigraniline, and was able to undergo the hydrolysis reaction. This degradation reaction is accompanied by a decrease of the peak intensity and by an increase of the peak width. Both have to be interpreted as an increase of the electrode resistance resulting from the polymer degradation. Finally, the greater loss of the specific capacity observed after thousands of cycles in 4 mol L^{-1} H_2SO_4 (when comparison is done with cycling performed in 1 mol L^{-1} H_2SO_4 solution) [41] can be explained by the values of the degradation kinetic constants we determined in this paper.

The degradation of the polymer is also observable in hydrochloric acid medium. However, the reaction kinetics is much lower than in sulfuric acid, as shown in Fig. 7. In a 1 mol L^{-1} HCl solution, k_{obs} is ca. 0.27×10^{-3} s^{-1}, and reaches the values 0.42×10^{-3} s^{-1} and 0.85×10^{-3} s^{-1} in 2 and 4 mol L^{-1} HCl, respectively. These values are three or four times lower than those obtained in H_2SO_4 for quite similar pH conditions. This shows that the counter ions associated with the proton play an important role during the hydrolysis. For the lower pH

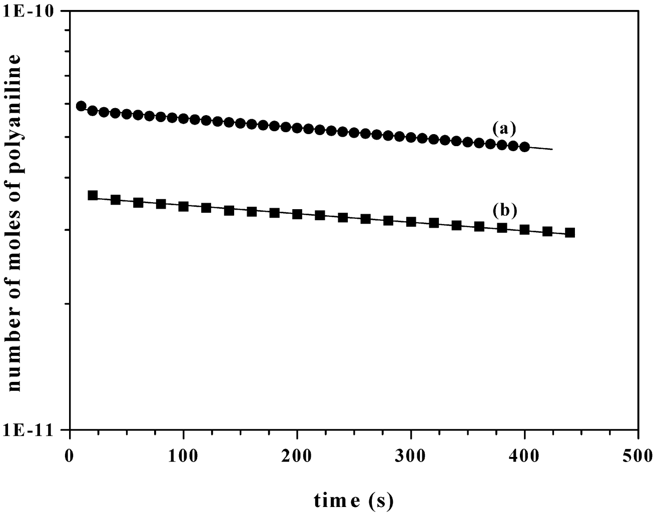

Fig. 5. Evolution of the number of moles of polyaniline versus the number of cycles: 50 mV s^{-1} (*a*) and 100 mV s^{-1} (*b*)

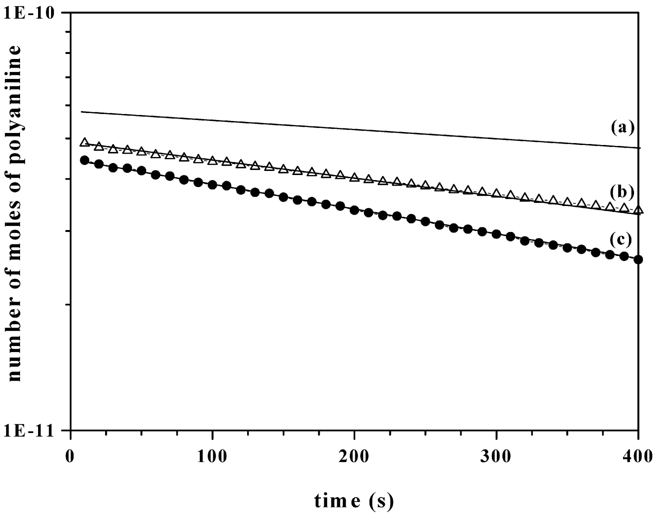

Fig. 6. Evolution of the number of moles of polyaniline versus the number of cycles at 50 mV s^{-1} in 0.5 mol L^{-1} H_2SO_4 (*a*), 1 mol L^{-1} H_2SO_4 (*b*), and 2 mol L^{-1} H_2SO_4 (*c*)

values in sulfuric acid medium, three ionic species should be taken into account: H^+, HSO_4^-, and SO_4^{2-}, suggesting that one of the latter two can also act as catalysts, like the H^+ ions. As a result, we can assume that, for battery applications, the use of hydrochloric acid as the electrolytic solution limits the degradation of the polymer.

Conclusions

The kinetics of PANi powder degradation in sulfuric and hydrochloric acids was successfully studied by cyclic voltammetry through a CME. It was shown that (1) the limiting process is a first-order kinetic reaction and (2) the degradation rate is acidic concentration dependent.

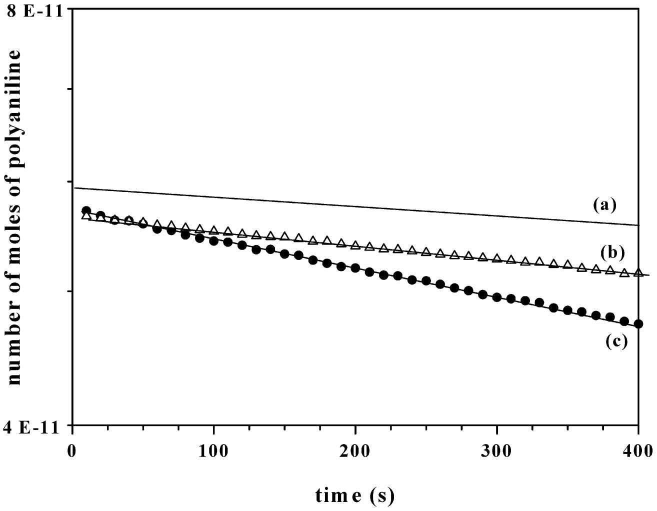

Fig. 7. Evolution of the number of moles of polyaniline versus the number of cycles at 50 mV s^{-1} in 1 mol L^{-1} HCl (*a*), 2 mol L^{-1} HCl (*b*), and 4 mol L^{-1} HCl (*c*)

The values of the kinetic constant were found to be quite different from those reported in the literature for thin films, but their evolution with respect to the acidic concentration was similar. A non-negligible difference of the degradation rate of PANi between sulfuric and hydrochloric acids was evidenced, leading to value at least three times higher in H_2SO_4 than in HCl. It was also shown that this degradation reaction can explain the specific capacity loss when PANi is used as a battery material.

References

1. Geniès EM, Boyle A, Lapkowski M, Tsintavis C (1990) Synth Met 36:139
2. Chao S, Wrighton M (1987) J Am Chem Soc 109:5526
3. Shinohara H, Chiba T, Aizawa M (1989) Sens Actuators 13:79
4. Desilvestro J, Scheifele W, Haas O (1992) J Electrochem Soc 139:2727
5. Osaka T, Ogano S, Naoi K, Oyama N (1989) J Electrochem Soc 136:306
6. Kitani A, Kaya M, Sasaki K (1986) J Electrochem Soc 133:1069
7. Green AG, Woodhead AE (1910) J Chem Soc 2388
8. Orata D, Buttry DA (1987) J Am Chem Soc 109:3574
9. Miras MC, Barbero C, Kötz R, Haas O (1994) J Electroanal Chem 369:193
10. Barbero C, Miras MC, Haas O, Kötz R (1991) J Electroanal Chem 310:437
11. Troise Frank MH, Denuault G (1994) J Electroanal Chem 379:399
12. Pruneanu S, Csahok E, Kertész V, Inzelt G (1998) Electrochim Acta 16–17:2305
13. Focke WJ, Wnek CE, Wei Y (1987) J Phys Chem 91:5813
14. Barbero C, Miras MC, Haas O, Kötz R (1991) J Electrochem Soc 138:669
15. Kalaji M, Peter LM, Abrantes LM, Mesquita JC (1989) J Electroanal Chem 274:289
16. Nyholm L, Peter LM (1994) J Chem Soc Faraday Trans 90:149
17. Andrieux CP, Audebert P, Hapiot P, Nechtschein N, Odin C (1991) J Electroanal Chem 305:153

18. Doriomedoff M, Cristofini FH, De Surville R, Josefowicz M, Yu LT, Buvet R (1971) J Chim Phys 68:1055
19. De Surville R, Josefowicz M, Yu LT, Perichon J, Buvet R (1968) Electrochim Acta 13:1451
20. Mermilliod N, Tanguy J, Hoclet M, Syed AA (1987) Synth Met 18:359
21. Macdiarmid AG, Mu S-L, Somasiri NLD, Wu W (1985) Mol Cryst Liq Cryst 121:187
22. Uchida I, Fujiyoshi H, Waki S (1997) J Power Sources 68:139
23. Perdicakis M, Grosselin N, Bessière J (1997) Electrochim Acta 42:3351
24. Scholz F, Lange B (1992) Trends Anal Chem 11:359
25. Fiedler DA (1998) J Solid State Electrochem 2:315
26. Vivier V, Cachet-Vivier C, Wu BL, Cha CS, Nedelec J-Y, Yu LT (1999) Electrochem Solid-State Lett 2:385
27. Vivier V, Cachet-Vivier C, Mezaille S, Wu BL, Cha CS, Nedelec J-Y, Fedoroff M, Michel D, Yu LT (2000) J Electrochem Soc 147:4252
28. Vivier V, Régis A, Sagon G, Nedelec J-Y, Yu LT, Cachet-Vivier C (2001) Electrochim Acta 46:907
29. Wightman RM (1981) Anal Chem 53:1125A
30. Dayton MA, Brown JC, Sttutts KJ, Wightman RM (1980) Anal Chem 52:946
31. Stilwell E, Park S-M (1988) J Electrochem Soc 135:2497
32. Stilwell DE, Park S-M (1989) J Electrochem Soc 136:688
33. Kazarinov VE, Andreev VN, Spitsyn MA (1996) Electrochim Acta 41:1760
34. Colomban P, Gruger A, Novak A, Regis A (1994) J Mol Struct 317:261
35. Gruger A, Novak A, Regis A, Colomban P (1994) J Mol Struct 328:153
36. Ohira M, Sakai T, Takeuchi M, Kobayashin Y, Tsuji M (1987) Synth Met 18:347
37. Baibarac M, Mihut L, Louarn G, Mevellec JY, Wery J, Lefrant S, Baltog I (1999) J Raman Spectrosc 30:1105
38. Hammett LP (1970) Physical organic chemistry, 2nd edn. McGraw-Hill, New York
39. Carlin C, Kepley LJ, Bard AJ (1985) J Electrochem Soc 132:353
40. Reeves RL (1962) J Am Chem Soc 84:3332
41. Vivier V, Cachet-Vivier C, Cha CS, Nedelec J-Y, Yu LT (2000) Electrochem Commun 2:180